# Characterization of the Thioether Product Formed from the Thiolytic Cleavage of the Alkyl−Nickel Bond in Methyl-Coenzyme M Reductase†

Ryan C. Kunz,‡ Mishtu Dey,‡ and Stephen W. Ragsdale*,‡,§

*Department of Biochemistry, University of Nebraska, Lincoln, Nebraska 68588, and Department of Biological Chemistry, University of Michigan, Ann Arbor, Michigan 48109-0606*

*Received September 25, 2007; Revised Manuscript Received December 18, 2007*

ABSTRACT: Methyl-coenzyme M reductase (MCR) catalyzes the terminal step in methanogenesis by using N-7-mercaptoheptanolyl-threonine phosphate (CoBSH) as the two-electron donor to reduce 2-(methylthiol)-ethane sulfonate (methyl-SCoM) to methane, and producing the heterodisulfide, CoBS-SCoM. The active site of MCR includes a noncovalently bound Ni tetrapyrrolic cofactor called coenzyme $F_{430}$, which is in the Ni(I) state in the active enzyme ($MCR_{red1}$). Bromopropanesulfonate (BPS) is a potent inhibitor and reversible redox inactivator that reacts with $MCR_{red1}$ to form an EPR-active state called $MCR_{PS}$, which is an alkyl−nickel species. When $MCR_{PS}$ is treated with free thiol containing compounds, the enzyme is reconverted to the active $MCR_{red1}$ state. In this paper, we demonstrate that the reactivation of $MCR_{PS}$ to $MCR_{red1}$ by thiols involves formation of a thioether product. $MCR_{PS}$ also can be converted to active $MCR_{red1}$ by treatment with sodium borohydride. Reactivation is highest with the smallest free thiol $HS^-$. Interestingly, $MCR_{PS}$ can also be reductively activated with analogues of CoBSH such as $CoB_8SH$ and $CoB_9SH$, but not CoBSH itself. Unambiguous demonstration of the formation of a methylthioether product from thiolysis of an alkyl−Ni species provides support for a methyl−Ni intermediate in the MCR-catalyzed last step in methanogenesis and the first proposed step in anaerobic methane oxidation.

Methanogens produce approximately 1 billion tons of methane per year (*1*). Methane is a relatively clean source of renewable energy, but it is also a greenhouse gas that is 20 times more potent than $CO_2$ (*2*). The terminal step in methanogenesis is catalyzed by methyl-coenzyme M reductase (MCR[1]), which uses N-7-mercaptoheptanolyl-threonine phosphate (CoBSH) as the two-electron donor to reduce 2-(methylthiol)ethane sulfonate (methyl-SCoM) to methane and the heterodisulfide CoBS-SCoM, eq 1 (*1*, *3*, *4*). MCR facilitates this reaction by employing a noncovalently bound nickel tetrapyrrolic cofactor called coenzyme $F_{430}$ (*5*−*7*), which is located at the bottom of a 30 Å hydrophobic active site channel in the enzyme (*8*).

$$\text{methyl-SCoM} + \text{CoBSH} \rightarrow \text{CH}_4 + \text{CoBS-SCoM}$$
$$\Delta G = -30\ \text{kJ/mol} \qquad (1)$$

The active form of the enzyme is known to have Ni in the +1 redox state; this state is referred to as $MCR_{red1}$ (*9*−*11*) (Figure 1). In addition to $MCR_{red1}$, two other states, $MCR_{PS}$ and $MCR_{ox1}$, may be relevant in the context of catalysis (Figures 1A and 1B, respectively). $MCR_{ox1}$ is best described as a Ni(III)/thiolate species in resonance with a Ni(II)/thiol radical species (*12*, *13*), which resembles the first intermediate in one of the proposed catalytic mechanisms described below. $MCR_{ox1}$ is generated *in vivo* by treating the actively growing cells with sodium sulfide or, alternatively, by switching the growth gas from $H_2/CO_2$ to $N_2/CO_2$ (*9*, *14*). $MCR_{ox1}$ can also be generated *in vitro* by treating $MCR_{red2}$ with polysulfide ($S_n$) (Figure 1B) (*15*). The second state of MCR that may be relevant for catalysis is $MCR_{PS}$, formerly called $MCR_{BPS}$ (eq 2 and Figure 1A) (*16*). $MCR_{PS}$ is an organometallic Ni(III)/propyl sulfonate species in resonance with a Ni(II)/propyl sulfonate radical (*17*), which resembles the first intermediate in a competing mechanistic proposal, described below. $MCR_{PS}$ is generated *in vitro* by treating $MCR_{red1}$ with BPS (*16*) or brominated acids (*18*).

BPS is the most potent inhibitor of MCR and has been described as an irreversible inhibitor (*19*), as a competitive inhibitor (*20*, *21*), and as shown in eqs 2−4, as a reversible redox inactivator (*22*). $MCR_{PS}$ and $MCR_{ox1}$ can be converted *in vitro* to $MCR_{red1}$. This is achieved by treating $MCR_{ox1}$ with the low potential reductant Ti(III) citrate ($E_0' = -0.66$ V) (*10*, *14*) or by reacting $MCR_{PS}$ with thiol containing compounds (eq 3) (*22*).

† This work was partly supported by a grant from the Department of Energy (S.W.R., DE-FG03-ER20297). The mass spectrometry instrumentation was purchased with funds from an NIH grant (1P20RR17675) to help support the Instrumentation Core of the Redox Biology Center at UNL.

* Corresponding author. Department of Biological Chemistry, University of Michigan, University of Michigan Medical School, 5301 MSRB III, 1150 W. Medical Center Drive, Ann Arbor, MI 48109-0606. Phone: (734) 615-4621. Fax: (734) 763-4581. E-mail: sragsdal@umich.edu.

‡ University of Nebraska.

§ University of Michigan.

[1] Abbreviations: MCR, methyl-coenzyme M reductase; methyl-SCoM, methyl-coenzyme M or 2-(methylthio)ethanesulfonate; HSCoM, coenzyme M or 2-thioethanesulfonate; $HSCoM_3$, 3-thiopropane-sulfonate; CoBSH, coenzyme B or N-7-mercaptoheptanoylthreonine phosphate; BPS, 3-bromopropane sulfonate; PS, propane sulfonate; BBS, 4-bromobutane sulfonate; NIM, negative ion mode; MS, mass spectrometry; NMR, nuclear magnetic resonance; $k_{max}$, apparent $k_{obs}$ maximum.

10.1021/bi701942w CCC: $40.75 
Published on Web 01/26/2008

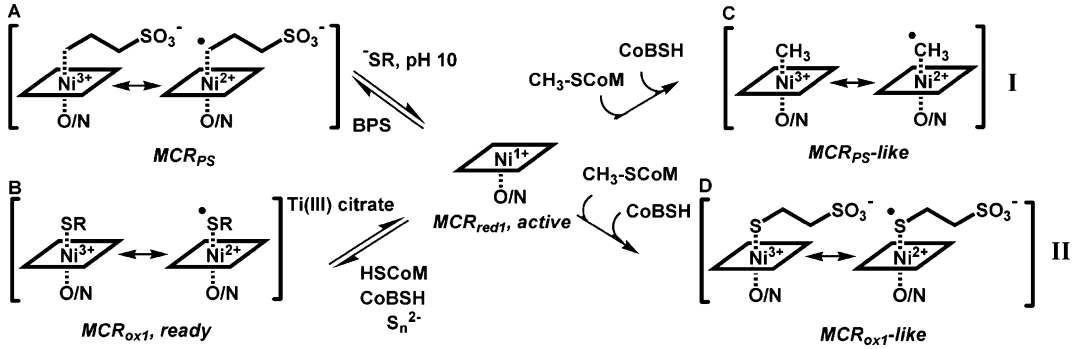


FIGURE 1: Relationship between (A) $MCR_{PS}$ and (C) the first proposed intermediate in mechanism I, and (B) $MCR_{ox1}$ and (D) the first proposed intermediate in mechanism II for methanogenesis. Coenzymes that do not ligate to $F_{430}$ are not shown.

Two mechanisms have been proposed for MCR, which can be distinguished by the first step of catalysis (Figures 1C and 1D). Mechanism I, based on the crystal structure (*8*) and studies of $F_{430}$ model complexes (*23*−*25*), proposes that the first step involves nucleophilic attack of Ni(I) of $F_{430}$ on the methyl group of methyl-SCoM, generating a methyl−Ni(III) intermediate ($MCR_{PS}$-like) (Figure 1C). Mechanism II is based on computational studies and proposes attack of Ni(I) on the sulfur atom adjacent to the methyl group of methyl-SCoM, promoting homolytic cleavage of the methyl−sulfur bond generating a Ni(III)−SCoM complex ($MCR_{ox1}$-like) and a methyl radical (Figure 1D) (*26*, *27*). The rationale for mechanism II is that the ∼45 kcal/mol difference in bond energy between the relatively strong C−S bond of methyl-SCoM and the relatively weak methyl−Ni(III) (first intermediate in mechanism I) would constitute an insurmountable thermodynamic barrier. It was calculated that the first step in mechanism II would have a less formidable energy barrier of only ∼20 kcal/mol.

Neither a true methyl−Ni(III) intermediate nor a Ni(III)−SCoM species has been observed upon reaction of $MCR_{red1}$ with the native substrate methyl-SCoM. Recently, it was shown that an alkyl−Ni(III) ($MCR_{PS}$) species is generated from the reaction of $MCR_{red1}$ with PS and other alkyl halides and that reaction of $MCR_{PS}$ with organic thiols can re-form the active $MCR_{red1}$ state (*22*). As shown in eq 3, it was proposed that a thioether product was formed during the conversion of the alkyl−Ni(III) species to $MCR_{red1}$.

$$MCR_{red1} + BPS \rightarrow Br^- + MCR_{PS} \quad (2)$$

$$MCR_{PS} + RS^- \rightarrow MCR_{red1} + RS\text{-}PS \quad (3)$$

$$MCR_{PS} + H^- \rightarrow MCR_{red1} + H\text{-}PS \quad (4)$$

Here we have characterized the reaction of $MCR_{PS}$ with thiol containing compounds and with a hydride donor to generate the active $MCR_{red1}$ state. By mass spectrometry (MS), it was shown that the product of the reactivation reaction with thiols is indeed a thioether sulfonate. Thus, this reaction resembles the reverse of the first step in mechanism I, the methylation of Ni(I) with methyl-CoM to generate a methyl−nickel bond. The kinetic data show that the efficiency for reactivation is highest with free thiols at pH 10.0. Interestingly, $MCR_{PS}$ can also be reactivated with analogues of CoBSH that are one ($CoB_8SH$) and two ($CoB_9$-SH) methylene group(s) longer than the native substrate, but not with CoBSH itself.

## MATERIALS AND METHODS

*Materials and Organism. Methanothermobacter marburgensis* was obtained from the Oregon Collection of Methanogens (Portland, OR) catalog as OCM82. All buffers, media ingredients, and other reagents were acquired from Sigma-Aldrich (St. Louis, MO) and, unless otherwise stated, were of the highest purity available. Solutions were prepared using Nanopure deionized water. $N_2$ (99.98%), $H_2S$ (99.0%), $H_2$/$CO_2$ (80%/20%), and Ultra High Purity (UHP) $H_2$ (99.999%) were obtained from Linweld (Lincoln, NE). Ti(III) citrate solutions were prepared from a stock solution of 200 mM Ti(III) citrate, which was synthesized by adding sodium citrate to Ti(III) trichloride (30 wt % solution in 2 N hydrochloric acid) (Acros Organics, Morris Plains, NJ) under anaerobic conditions and adjusting the pH to 7.0 with sodium bicarbonate (*28*). The concentration of Ti(III) citrate was determined routinely by titrating a methyl viologen solution.

*Synthesis of Methyl-SCoM, CoBSH, $CoB_8SH$, and $CoB_9SH$.* Methyl-SCoM was prepared from HSCoM and methyl iodide (*29*). CoBS-SCoB, $CoB_8S$-$SCoB_8$, and $CoB_9S$-$SCoB_9$ were prepared as described from 7-bromoheptanoic acid (Karl Industries, Aurora, OH), 8-bromooctanoic acid, and 9-bromononanoic acid (Matrix Scientific, Columbia, SC), respectively (*30*, *31*). The free thiol forms of CoBSH, $CoB_8SH$ and $CoB_9SH$ were generated by the reduction of the homodisulfides CoBS-SCoB, $CoB_8S$-$SCoB_8$, and $CoB_9S$-$SCoB_9$, respectively. The reduction was carried out in 25% concentrated formic acid using a 3-fold molar excess of Tris (2-carboxyethyl) phosphine hydrochloride (TCEP) (Pierce, Rockford, IL) over the homodisulfide concentration, as described by the manufacturer. Reduced CoBSH (or its analogues) was separated from the homodisulfide by HPLC. The homodisulfide/TCEP reaction was loaded onto a 7.8 × 300 mm $\mu$Bondapak C18 column (Waters, Milford, MA) at 3 mL/min, equilibrated with aqueous 0.1% trifluoroacetic acid (TFA) and developed with a linear gradient from 0 to 90% ACN in 0.1% TFA over 30 min. The buffer reservoirs for the HPLC were purged with high purity $N_2$ to minimize the oxidation of CoBSH (or analogues) during HPLC purification. CoBSH, $CoB_8SH$, and $CoB_9SH$ eluted at 13%, 17%, and 22% ACN, respectively, and were collected in 9 mL anaerobic serum vials (Alltech Inc., Deerfield, IL) fitted with rubber butyl septa (Bellco Inc., Vineland, NJ). The anaerobic CoBSH (or analogue) solution was titrated with DTNB to determine the concentration of the reduced thiols (*31*). The purity of methyl-SCoM, CoBSH, $CoB_8SH$, and $CoB_9SH$ was ascertained to be >90% by $^1H$ NMR.

*Mt. marburgensis Growth, Harvest and $MCR_{red1}$ Purification Conditions.* $MCR_{red1}$ was isolated from *Mt. marburgensis* cultured on $H_2/CO_2/H_2S$ (80%/20%/0.1%) at 65 °C in a 14 L fermentor (New Brunswick Scientific Co., Inc. New Brunswick, NJ) (*10*, *32*). Culture media were prepared as previously described (*32*). $MCR_{red1}$ was generated *in vivo* and purified as described earlier (*22*). The purification procedure routinely generates 60−70% $MCR_{red1}$ as determined by UV−visible and EPR spectroscopy as described earlier (*22*).

*Spectroscopy of MCR.* UV−visible spectra of MCR were recorded in the anaerobic chamber using a diode array spectrophotometer (model DT 1000A, Analytical Instrument Systems, Inc., Flemingron, NJ). EPR spectra were recorded on a Bruker EMX spectrometer (Bruker Biospin Corp., Billerica, MA), equipped with an Oxford ITC4 temperature controller, a Hewlett-Packard model 5340 automatic frequency counter, and Bruker gaussmeter. Unless otherwise noted, the EPR spectroscopic parameters included the following: temperature, 70 K; microwave power, 10 mW; microwave frequency, 9.43 GHz; receiver gain, $2 \times 10^4$; modulation amplitude, 5.0 G; modulation frequency, 100 kHz. Double integrations of the EPR spectra were performed and referenced to a 1 mM copper perchlorate standard. All NMR data were acquired at 298 K on a Bruker Avance DRX 500 MHz NMR instrument equipped with a TXI cryoprobe in the UNL Chemistry Department.

*Stopped-Flow Studies.* Stopped-flow experiments were carried out on an Applied Photophysics spectrophotometer (SX.MV18, Leatherhead, U.K.) equipped with a photodiode array detector. Rigorous measures were taken to remove oxygen from the stopped-flow instrument. Buffered solutions of enzymes and inhibitors were made in the anaerobic chamber. All buffered solutions contained 0.2 mM Ti(III) citrate as an oxygen scavenger, since attempts to exclude Ti(III) citrate from the buffers resulted in oxidation of the $O_2$-labile $MCR_{red1}$ and $MCR_{PS}$ species. The solutions were loaded into tonometers, which had been incubated in the anaerobic chamber for 4 days and served as reservoirs for the drive syringes of the stopped-flow instrument. The drive syringes and mixing chamber were made anaerobic by flushing the chamber with a dithionite:resazurin (1 mM:0.02 mM) solution in 0.1 M NaOH. $MCR_{PS}$ and varied concentrations of thiolates were rapidly mixed at 25 °C in a 1:1 ratio. The reaction was monitored in the single wavelength mode by following the increase of $MCR_{red1}$ at 385 nm, using a 1 cm path length cell. Data were fit to a single-exponential decay function with software provided by Applied Photophysics (version SX MV.18). Reported rate constants are the average of at least three different rapid-mixing experiments.

*Mass Spectrometry.* All mass spectra (MS) were collected in the negative ion mode by direct infusion to a 4000 Qtrap (ABS) mass spectrometer using a kD Scientific microflow syringe pump. The data was acquired and processed using Analyst 1.4.1 software. Data was acquired in Q1 (quadrupole one) and product ion scan in negative ion mode. The mass range of 50−300 amu (atomic mass units) was scanned in 1 s. The ion spray voltage was set to −4500 V, the temperature was set to 22 °C and a declustering potential (DP) value was −50 V. $MCR_{red1}$ was incubated for 5 min with 10-fold excess of BPS in 50 mM Tris-HCl, pH 7.6. Unreacted BPS was removed from $MCR_{PS}$ by buffer exchange using an Amicon Ultra-15 centrifuge filter with a 50 kDa cutoff (Millipore, Bedford, MA). Typically, 300−600 $\mu$L of $MCR_{PS}$/BPS reaction mixture was exchanged into 3−6 mL of 50 mM Tris-HCl pH 7.6 containing 0.1 mM Ti(III) citrate. This mixture was concentrated to 200−300 $\mu$L, and this process was repeated three times. The concentration of $MCR_{PS}$ was determined by EPR spectroscopy. $MCR_{PS}$ was reactivated with various thiols (see figure legend(s)) for more details) and the reactivation reaction was monitored for completion using UV−visible spectroscopy. Once the reaction was complete, enzyme and ligands were separated using a 0.5 mL Microcon centrifugal filter device with a 30 kDa cutoff filter (Millipore). All MS samples were prepared by mixing the ligand solution with an equal volume of acetonitrile/water (50%/50%).

## RESULTS

*Conversion of $MCR_{PS}$ to $MCR_{red1}$ by Free Thiols.* In a previous manuscript, we presented evidence for the two-electron reductive reactivation of $MCR_{PS}$ to $MCR_{red1}$ using HSCoM as the electron donor (*22*). In addition, we showed that other thiol containing compounds could participate in this reactivation reaction. Here we present a more detailed assessment of the kinetics for the reactivation of $MCR_{PS}$ with various free thiol containing compounds to generate active $MCR_{red1}$. As reported earlier, $MCR_{PS}$ is reactivated by HSCoM with a $k_{max}$ of 0.0092 $s^{-1}$ and $K_M$ of 3.5 mM (*22*), which is similar to its inhibition constant in methane formation ($K_i = 4$ mM, (*19*)). The second-order rate constant for the reaction is 2.6 $M^{-1}$ $s^{-1}$. Changing the length of HSCoM had little effect on the reactivation kinetics, since the second-order rate constant for reactivation is 2.9 $M^{-1}$ $s^{-1}$ with 3-mercaptopropane sulfonate ($HSCoM_3$) (Figure S1, Supporting Information).

Previously, we observed that CoBSH was unable to reactivate $MCR_{PS}$ (*22*). This lack of activity is likely because CoBSH is securely anchored to the top of the active site by its threonine phosphate group, which places its thiol group ~6.5 Å from the sulfur atom of HSCoM in the $MCR_{ox1-silent}$ structure (*8*). This should approximate the distance between the thiol group of CoBSH and the methylene group of propyl sulfonate (PS) covalently attached to the Ni atom of $F_{430}$. This ~6.5 Å gap would prevent formation of a thioether linkage, unless there are conformational changes that would allow CoBSH to reach deeper into the active site. In the absence of a conformational change, one strategy to bridge this 7 Å gap could be achieved by increasing the aliphatic arm length of CoBSH, which in turn would allow analogues of CoBSH to reactivate $MCR_{PS}$. To accomplish this, we synthesized analogues of CoBSH that are 1 and 2 methylene group(s) longer, generating $CoB_8SH$ and $CoB_9SH$, respectively. Each successive methylene group should allow the $CoB_xSH$ ($x$ = the number of carbon atoms in the aliphatic arm) analogue to reach ~2 Å deeper into the active site. Accordingly, $CoB_8SH$ (Figure 2) and $CoB_9SH$ (Figure S2, Supporting Information) can reactivate $MCR_{PS}$ to $MCR_{red1}$, with $CoB_8SH$ exhibiting about a 13-fold higher second-order rate constant than $CoB_9SH$. The $k_{max}$ for $CoB_8SH$ is 0.0026 $s^{-1}$, which is 4-fold lower than that for the HSCoM analogues; however, the $k_{max}/K_M$ is larger since the $K_M$ for $CoB_8SH$ is relatively low (0.016 mM). This $K_M$ value is

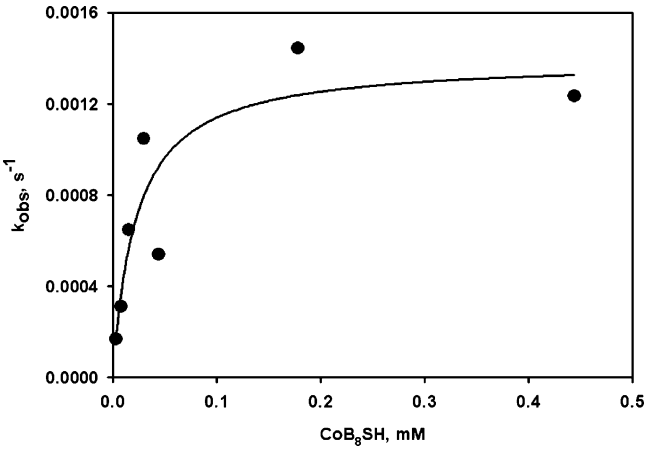


FIGURE 2: Determination of the second-order rate constant for the conversion of $MCR_{PS}$ to $MCR_{red1}$ by $CoB_8SH$. The reactions were monitored at 385 nm with UV−visible spectroscopy. 8.1 $\mu$M $MCR_{red1}$ was converted to $MCR_{PS}$ by the addition of 40 $\mu$M BPS in 0.5 M TAPS-Na + 0.1 mM Ti(III) citrate, pH 10.0 at 25 °C. Different concentrations of $CoB_8SH$ were added to start the reactivation reactions. The data were fit to a 2-parameter hyperbolic equation with a $k_{max}$ of 0.084 ± 0.013 $min^{-1}$, a $K_M$ of 0.022 ± 0.012 mM, and a second-order rate constant of 64 ± 37 $M^{-1}$ $s^{-1}$.

Table 1: Kinetic Parameters for the Reactivation of $MCR_{PS}$ to $MCR_{red1}$ Using Various Thiols as Reductants[a]

| substrate | $K_M$ (mM)[b] | $k_{max}$ ($s^{-1}$)[b] | $k_{max}/K_M$ ($M^{-1}$ $s^{-1}$)[b] |
|---|---|---|---|
| HSCoM | 3.5 ± 1.0 | 0.0092 ± 0.0026 | 2.6 ± 1.0 |
| $HSCoM_3$ | 62 ± 19 | 0.18 ± 0.14 | 2.9 ± 2.4 |
| $CoB_8SH$ | 0.016 ± 0.008 | 0.0026 ± 0.0012 | 160 ± 134 |
| $CoB_9SH$[c] | 0.46 ± 0.22 | 0.0054 ± 0.001 | 12 ± 6 |
| 2-mercaptoethanol[c] | 50 ± 4 | 0.65 ± 0.02 | 13 ± 1 |
| DTT[c] | 75 ± 3 | 0.16 ± 0.01 | 2.1 ± 0.2 |
| cysteine | 16 ± 5.8 | 8.8 ± 1.6 | 550 ± 230 |
| $Na_2S$ | 8.8 ± 2.1 | 14 ± 2.8 | 1600 ± 500 |

[a] All experiments were performed at 25 °C and pH 10.0. [b] All values and standard deviations were calculated from at least two independent experiments using different enzyme preparations unless indicated otherwise. [c] These concentration dependence experiments were conducted once.

similar to its inhibition constant in methane formation ($K_i$ = 15 $\mu$M, (*33*)). The overall second-order rate constant for $CoB_8SH$ in converting $MCR_{PS}$ to $MCR_{red1}$ is 160 $M^{-1}$ $s^{-1}$, while, for $CoB_9SH$, the $k_{max}$ is 0.0054 $s^{-1}$ and the $K_M$ is 0.463 mM, giving a second-order rate constant of 12 $M^{-1}$ $s^{-1}$. One might expect $CoB_9SH$ to be a better reactivating molecule than $CoB_8SH$ since the thiol group of $CoB_9SH$ will be able to reach further into the active site than $CoB_8SH$. However, the close proximity of the thiol to the nickel may pose steric hindrance, reducing the activity of the thiol of $CoB_9SH$ in nucleophilic attack on the carbon bound to nickel.

Other thiol containing compounds can reactivate $MCR_{PS}$ to $MCR_{red1}$ (Table 1). Surprisingly, 2-mercaptoethanol and cysteine (Figure 3) exhibit high values of $k_{max}$, even faster than the $k_{cat}$ for methane formation with methyl-SCoM and CoBSH (4.4 $s^{-1}$ at 20 °C) and 2 orders of magnitude better than HSCoM. Furthermore, their relatively low affinities for the MCR active site are only slightly lower than those for HSCoM and $HSCoM_3$ (Figure S3, Supporting Information). Conversely, DTT exhibits both a relatively low affinity and slow reactivity (Figure S4, Supporting Information).

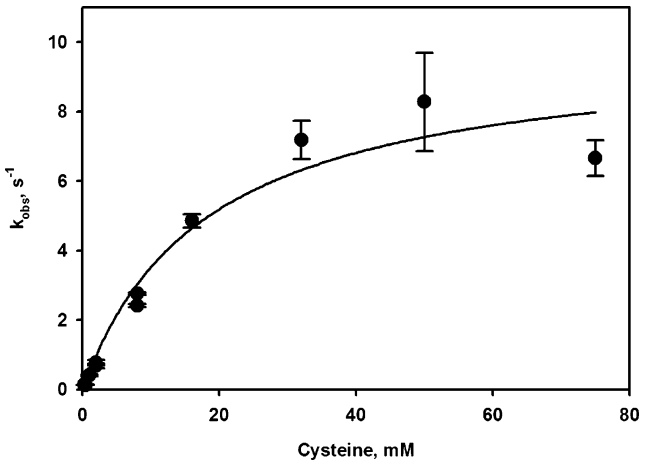


FIGURE 3: Determination of the second-order rate constant for the conversion of $MCR_{PS}$ to $MCR_{red1}$ with cysteine as reductant. The reactions were monitored at 385 nm using stopped-flow UV−visible spectroscopy. 20 $\mu$M $MCR_{red1}$ was converted to $MCR_{PS}$ by the addition of 120 $\mu$M BPS in 0.5 M TAPS-Na and 0.2 mM Ti(III) citrate, pH 10.0 (syringe 1). Different concentrations of cysteine in 0.5 M TAPS-Na and 0.2 mM Ti(III) citrate, pH 10 (syringe 2), were used to start the reactions. All experiments were done at 25 °C. The data was fit to a 2-parameter hyperbolic equation with a $k_{max}$ of 9.9 ± 1.1 $s^{-1}$, $K_M$ of 18 ± 5 mM, and a second-order rate constant of 540 ± 160 $M^{-1}$ $s^{-1}$.

The smallest free thiol we tested was $HS^-$ (from $Na_2S$) (Figure S5, Supporting Information). This compound exhibits a high catalytic efficiency for reactivation, 1600 $M^{-1}$ $s^{-1}$, which may reflect its small size and hence unhindered access to the active site of MCR. Unlike all other reactivating thiol containing compounds tested, $HS^-$ could reactivate $MCR_{PS}$ at pH 10 and 7.6, exhibiting a much wider pH range for reactivation than the other thiols tested.

*$MCR_{PS}$ Is Reactivated to $MCR_{red1}$ by $NaBH_4$.* The reactivation of $MCR_{PS}$ using various thiols could be considered a two-electron reduction of the Ni center (Ni(III) to Ni(I)) or a nucleophilic attack, so we reasoned that hydride ion (from $NaBH_4$) should be able to perform the same chemistry as that of the thiol containing compounds and generate an alkane sulfonate. The reactivation of $MCR_{PS}$ with ~4 mM $NaBH_4$ at pH 10 is shown in Figure 4. It is difficult to accurately determine a second-order rate constant for reduction of $MCR_{PS}$ to $MCR_{red1}$ by $NaBH_4$ because of the inaccuracy in determining the concentration of hydride ion in solution, since hydride is rapidly protonated in solution. However, the second-order rate constant estimated from the observed value of the rate constant with 4 mM $NaBH_4$ is approximately 6 $M^{-1}$ $s^{-1}$. While $NaBH_4$ is effective at reducing $MCR_{PS}$ to $MCR_{red1}$, the one-electron reductant Ti(III) citrate is very sluggish and leads predominantly to an EPR silent Ni(II) state with less than 10% conversion to $MCR_{red1}$, as described earlier (*22*).

*Mass Spectrometric Evidence That a Thioether Is Formed from the Reaction of $MCR_{PS}$ and HS-R.* We used MS to identify the products from the reaction between $MCR_{PS}$ and several of the thiols listed in Table 1. When $MCR_{PS}$ was reacted with cysteine, a peak in negative ion mode (NIM) was observed at *m*/*z* 242.2 that corresponds to the molecular formula $C_6H_{13}O_5NS_2$ with an exact mass of 243. This can be assigned to a thioether product, Cys-S-PS (3-(2-amino,3-thiopropionate) propane sulfonic acid). Peaks due to unre-

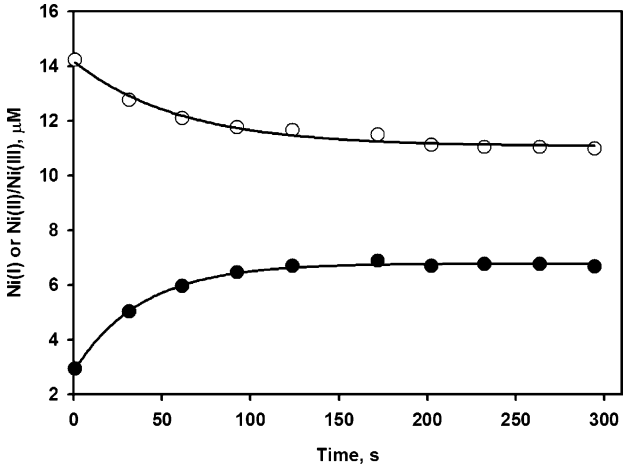


FIGURE 4: Conversion of $MCR_{PS}$ to $MCR_{red1}$ with $NaBH_4$. The reaction was monitored with UV−visible spectroscopy. 12 $\mu$M $MCR_{PS}$ was mixed with 4 mM $NaBH_4$ in 0.5 M TAPS-Na + 0.1 mM Ti(III) citrate, pH 10 at 25 °C. The data was fit with a 3-parameter single-exponential equation. The observed rate constants are $0.026 \pm 0.001$ $s^{-1}$ (at 385 nm, Ni(I): closed circles) and $0.017 \pm 0.002$ $s^{-1}$ (420 nm, Ni(II)/Ni(III): open circles).

acted cysteine and cysteine homodisulfide (cystine) appear at *m*/*z* 120.1 and 238.8, respectively (inset, Figure 5A). MS/MS analysis of the parent ion peak at *m*/*z* 242.2 yielded the fragmentation pattern shown in Figure 5A. The daughter ion observed at *m*/*z* 155.3 (peak labeled "b" in Figure 5A) is assigned to 3-mercaptoate propane sulfonic acid, the fragment where the thioether (C−S) bond is cleaved on the cysteine side of the thioether group. The other daughter ion, desulfocysteine (alanine), is probably neutral and cannot be detected in NIM. The daughter ion at *m*/*z* 120.0, peak labeled "a" in Figure 5A, is assigned to the fragment when the thioether (S−C) bond is cleaved to form cysteine.

The fragmentation pattern in both the MS and MS/MS modes for $^{13}$C-cysteine is nearly identical to that of cysteine. The inset in Figure 5B shows the MS spectrum of the ligand solution when $^{13}$C-cysteine is used to reactivate $MCR_{PS}$. $^{13}$C-Cysteine is observed at *m*/*z* 121.0, as expected, 1 mass unit larger than cysteine (inset to Figure 5A). Similarly, $^{13}$C-Cystine (*m*/*z* = 241.0) is two mass units higher than $^{12}$C-cystine. $^{13}$C-Cysteine reacts with $MCR_{PS}$ to give the product $^{13}$C-Cys-S-PS, which has an exact mass of 244 and appears at *m*/*z* 243.1. This is one mass unit higher than $^{12}$C-Cys-S-PS. To validate the assignment as $^{13}$C-Cys-S-PS, MS/MS was performed on the peak at *m*/*z* 243.1 (Figure 5B). Fragmentation of the parent ion peak with *m*/*z* 243.1 gives rise to daughter ions. The peak at *m*/*z* 155.2 (peak labeled "b" in Figure 5B) is assigned to the fragment when the $^{13}$C−S bond is cleaved at the $^{13}$C-cystine side of the thioether group, 3-mercaptoate propane sulfonic acid. Similarly, the thioether (S−C) bond can cleave on the propane sulfonate side to yield the daughter ion that has been assigned as $^{13}$C-cysteine having *m*/*z* 121.0, peak labeled "a" in Figure 5B.

MS/MS analysis was also used to identify the thioether products for the reaction of $MCR_{PS}$ with HSCoM (Figure S6), $HSCoM_3$ (Figure S7), and 2-mercaptoethanol (Figure S8) (Supporting Information). Based on the MS data, we are confident that the reaction of $MCR_{PS}$ with these thiols generates a thioether product.

## DISCUSSION

Rapid reaction studies of MCR with the natural substrates have not led to the identification of any intermediates in the catalytic cycle. Thus, two crucial remaining questions related to the prodigious activity of MCR are (1) what are the key catalytic intermediates in the mechanism of this enzyme and (2) how is the active form of MCR generated and maintained. Our studies on $MCR_{PS}$ address aspects of these two key questions. Although reaction of MCR with the natural substrates have not led to measurable changes in the EPR or UV−visible spectra of $MCR_{red1}$, studies with the substrate analogue BPS lead to the formation of an alkyl−Ni(III) intermediate ($MCR_{PS}$) that can undergo conversion back to the $MCR_{red1}$ state. These steps are analogous to those proposed for mechanism I in methane formation. In addition, until recently, $MCR_{ox1}$ was the only form of the enzyme that was known to undergo activation to form $MCR_{red1}$ *in vitro*. It was recently recognized that $MCR_{PS}$, which had been classified as an irreversible inhibitor (*19*), is a redox inactivator whose inhibitory activity can be reversed by conversion of MCR back to the active $MCR_{red1}$ state.

This manuscript describes the characterization of the conversion of $MCR_{PS}$ to $MCR_{red1}$ by thiol containing compounds (Table 1) and by sodium borohydride. Both of these reactions involved nucleophilic displacement of the alkyl sulfonate from its organometallic complex with Ni(III). In an earlier study we suggested that a thioether would be formed as the product of the thiol-dependent reactivation reaction. Using MS analysis, thioether products have been unambiguously identified from the reaction of $MCR_{PS}$ with several thiols. In each case, the product contains the thiol nucleophile attached to propyl sulfonate, i.e., RS-propyl sulfonate.

Given that both $MCR_{ox1}$ and $MCR_{PS}$ can undergo activation to $MCR_{red1}$, it is perhaps not surprising that they share similar electronic properties. However, the activation conditions differ markedly. The conversion of the alkyl−Ni ($\Delta H \sim 25$ kcal/mol) species in $MCR_{PS}$ to $MCR_{red1}$ appears to involve a one-step, two-electron reduction delivered *via* a thiolate or hydride to generate a thioether sulfonate (a carbon−sulfur bond, $\Delta H \sim 70$ kcal/mol) or an alkyl sulfonate (carbon−hydrogen bond, $\Delta H \sim 100$ kcal/mol) product, respectively (eqs 3 and 4) (*26*). Thus, these are highly favorable reactions. While two-electron nucleophilic reactions are excellent at reactivating $MCR_{PS}$, the strongly reducing one-electron reductant, Ti(III) citrate, is not efficient at reducing $MCR_{PS}$ to $MCR_{red1}$ and leads predominantly to an inactive Ni(II) state (*22*). On the other hand, Ti(III) citrate is an excellent reductant for $MCR_{ox1}$, converting it nearly quantitatively to $MCR_{red1}$ (*10*, *14*). For many years, this was the only known way to generate "high" activity $MCR_{red1}$ *in vitro*. However, neither $NaBH_4$ nor thiolates are effective in converting $MCR_{ox1}$ to the active $MCR_{red1}$ state in spite of the apparently favorable thermodynamics of cleaving a Ni−thiolate ($\Delta H \sim 40$ kcal/mol) to generate a disulfide ($\Delta H \sim 60$ kcal/mol) (*26*).

Thus, it is apparently not only the thermodynamics of forming the thioether versus the disulfide that explains the varying requirements for activating $MCR_{PS}$ and $MCR_{ox1}$, respectively. It appears likely that the differences derive from the differences in the electronic structures of the two species

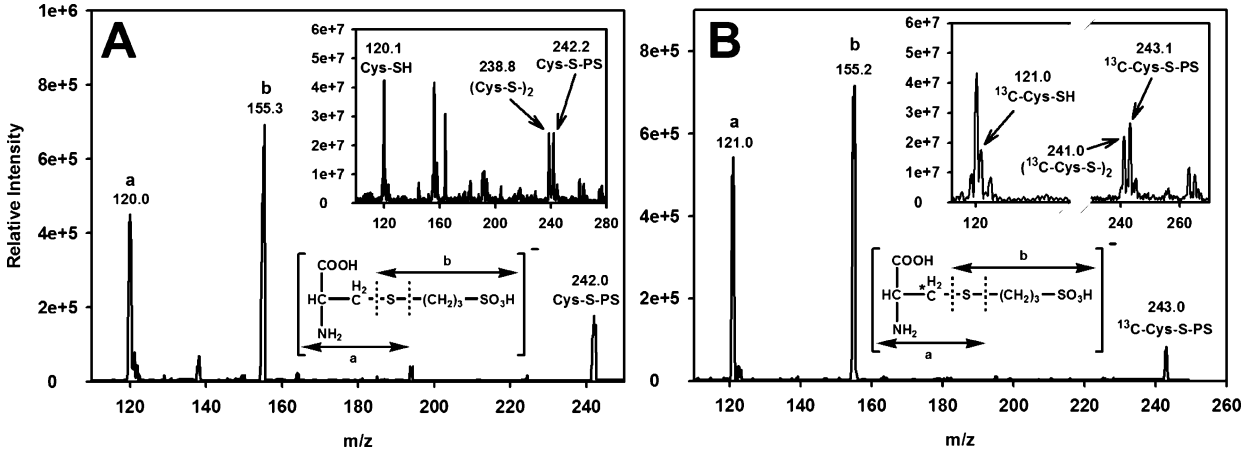


FIGURE 5: NIM-MS/MS spectrum of the reaction mixture from the $MCR_{PS}$ reactivation using cysteine as a reductant. 126 $\mu$M $MCR_{PS}$ was reacted with 2 mM cysteine (A) or 2 mM $^{13}$C-cysteine (B) in 200 mM ammonium carbonate, pH 10.0 (see Materials and Methods for MS sample preparation). Inset: NIM-MS spectrum of the reaction mixture. *The position of the $^{13}$C-label on Cys.

(Figure S9, Supporting Information). The spin density distributions for $MCR_{ox1}$ and $MCR_{PS}$ are similar, with approximately 75% unpaired spin residing on Ni and about 7% on the methylene carbon of $MCR_{PS}$ (*17*, *34*, *35*) or thiolate sulfur of $MCR_{ox1}$ (*13*). However, the alkyl group in the $MCR_{PS}$ complex is relatively electrophilic, favoring nucleophilic attack by a thiolate or hydride, while the sulfur in $MCR_{ox1}$ would have more radical character, favoring one-electron reactions. Thus, since Ti(III) citrate is an obligate one-electron donor, the reduction of $MCR_{ox1}$ by Ti(III) citrate would presumably proceed *via* two, one-electron reduction steps.

It is somewhat surprising that a range of thiolates, including $CoB_8SH$ and $CoB_9SH$, can facilitate the reductive activation of $MCR_{PS}$, however CoBSH cannot. This apparent contradiction may reflect a strong steric bias in the MCR active site that prevents the natural substrate CoBSH from performing a nucleophilic attack on the alkyl−Ni intermediate. In the context of mechanism I, such a reaction would short-circuit methanogenesis and lead to the formation of CoBS-methyl, a potent inhibitor of MCR (*33*). Although this reaction would regenerate $MCR_{red1}$, it would deplete the cellular pool of CoBSH, inhibit methane synthesis, and prevent heterodisulfide formation, the reduction of which is coupled to cellular energy production. That $CoB_8SH$ and $CoB_9SH$ can reactivate $MCR_{PS}$ to generate a $CoB_xS$-PS product must reflect a very fine tuning of the active site to keep the sulfur of CoBSH out of reach of the upper axial Ni ligand.

The observations that CoBSH is unable to reactivate $MCR_{PS}$ and that thiols are unable to convert $MCR_{ox1}$ to $MCR_{red1}$ appear inconsistent with mechanism II, since this mechanism proposes that a thiyl-radical (from CoBSH) attacks a $MCR_{ox1}$-like species (Ni-SR) to generate a disulfide anion radical (CoBS-SCoM). However, these experiments do not strictly rule out mechanism II, which involves reaction of the CoBS thiyl-radical with a Ni(II)-thiolate, instead of a thiolate with a Ni(III)-thiolate (in the case of $MCR_{ox1}$) and of a thiolate with an alkyl−Ni(III) (in the case of $MCR_{PS}$). On the other hand, identification of the products of the reaction of $MCR_{PS}$ with free thiols or with hydride does provide support for mechanism I, since in the first reaction in anaerobic methane oxidation by reverse methanogenesis, methane would be converted to the alkyl−Ni state ($MCR_{PS}$), which would react with CoM to generate $MCR_{red1}$ and a thioether sulfonate (methyl-SCoM). These steps are the reverse of the reactions involved in the last step in methanogenesis.

## ACKNOWLEDGMENT

We thank Dr. Ashraf Raza for assistance in running mass spectrometric experiments.

## SUPPORTING INFORMATION AVAILABLE

Nine figures showing kinetic and mass spectroscopic data for the formation of $MCR_{red1}$ by reacting $MCR_{PS}$ with various thiols. This material is available free of charge via the Internet at http://pubs.acs.org.

## REFERENCES

1. Thauer, R. K. (1998) Biochemistry of methanogenesis: a tribute to Marjory Stephenson. 1998 Marjory Stephenson Prize Lecture, *Microbiology 144* (Part 9), 2377−2406.
2. Ragsdale, S. W. (2003) *Biochemistry of Methylcoenzyme M Reductase and Coenzyme F430*, Vol. 11, Academic Press, New York.
3. DiMarco, A. A., Bobik, T. A., and Wolfe, R. S. (1990) Unusual coenzymes of methanogenesis, *Annu. Rev. Biochem. 59*, 355−394.
4. Ellermann, J., Kobelt, A., Pfaltz, A., and Thauer, R. K. (1987) On the role of N-7-mercaptoheptanoyl-O-phospho-L-threonine (component B) in the enzymatic reduction of methyl-coenzyme M to methane, *FEBS Lett. 220*, 358−362.
5. Diekert, G., Jaenchen, R., and Thauer, R. K. (1980) Biosynthetic evidence for a nickel tetrapyrrole structure of factor F430 from Methanobacterium thermoautotrophicum, *FEBS Lett. 119*, 118−120.
6. Diekert, G., Klee, B., and Thauer, R. K. (1980) Nickel, a component of factor F430 from Methanobacterium thermoautotrophicum, *Arch. Microbiol. 124*, 103−106.
7. Whitman, W. B., and Wolfe, R. S. (1980) Presence of nickel in factor F430 from Methanobacterium bryantii, *Biochem. Biophys. Res. Commun. 92*, 1196−1201.
8. Ermler, U., Grabarse, W., Shima, S., Goubeaud, M., and Thauer, R. K. (1997) Crystal structure of methyl-coenzyme M reductase: the key enzyme of biological methane formation, *Science 278*, 1457−1462.
9. Albracht, S. P. J., Ankel-Fuchs, D., Böcher, R., Ellermann, J., and Moll, J., van der Zwann, J. W., and Thauer, R. K. (1988) Five new EPR signals assigned to nickel in methyl-coenzyme M reductase from Methanobacterium thermoautotrophicum, strain Marburg, *Biochim. Biophys. Acta 955*, 86−102.

10. Goubeaud, M., Schreiner, G., and Thauer, R. K. (1997) Purified methyl-coenzyme-M reductase is activated when the enzyme-bound coenzyme F430 is reduced to the nickel(I) oxidation state by titanium(III) citrate, *Eur. J. Biochem. 243*, 110−114.
11. Rospert, S., Bocher, R., Albracht, S. P., and Thauer, R. K. (1991) Methyl-coenzyme M reductase preparations with high specific activity from H2-preincubated cells of Methanobacterium thermoautotrophicum, *FEBS Lett. 291*, 371−375.
12. Craft, J. L., Horng, Y. C., Ragsdale, S. W., and Brunold, T. C. (2004) Nickel oxidation states of F(430) cofactor in methyl-coenzyme M reductase, *J. Am. Chem. Soc. 126*, 4068−4069.
13. Harmer, J., Finazzo, C., Piskorski, R., Bauer, C., Jaun, B., Duin, E. C., Goenrich, M., Thauer, R. K., Van Doorslaer, S., and Schweiger, A. (2005) Spin density and coenzyme M coordination geometry of the ox1 form of methyl-coenzyme M reductase: a pulse EPR study, *J. Am. Chem. Soc. 127*, 17744−17755.
14. Becker, D. F., and Ragsdale, S. W. (1998) Activation of methyl-SCoM reductase to high specific activity after treatment of whole cells with sodium sulfide, *Biochemistry 37*, 2639−2647.
15. Mahlert, F., Bauer, C., Jaun, B., Thauer, R. K., and Duin, E. C. (2002) The nickel enzyme methyl-coenzyme M reductase from methanogenic archaea: In vitro induction of the nickel-based MCR-ox EPR signals from MCR-red2, *J. Biol. Inorg. Chem. 7*, 500−513.
16. Rospert, S., Voges, M., Berkessel, A., Albracht, S. P., and Thauer, R. K. (1992) Substrate-analogue-induced changes in the nickel-EPR spectrum of active methyl-coenzyme-M reductase from Methanobacterium thermoautotrophicum, *Eur. J. Biochem. 210*, 101−107.
17. Hinderberger, D., Piskorski, R. P., Goenrich, M., Thauer, R. K., Schweiger, A., Harmer, J., and Jaun, B. (2006) A nickel-alkyl bond in an inactivated state of the enzyme catalyzing methane formation, *Angew. Chem., Int. Ed. Engl. 45*, 3602−3607.
18. Dey, M., Kunz, R. C., Lyons, D. M., and Ragsdale, S. W. (2007) Characterization of Alkyl-Nickel Adducts Generated by Reaction of Methyl-Coenzyme M Reductase with Brominated Acids, *Biochemistry, 46*, 11969−11978.
19. Goenrich, M., Mahlert, F., Duin, E. C., Bauer, C., Jaun, B., and Thauer, R. K. (2004) Probing the reactivity of Ni in the active site of methyl-coenzyme M reductase with substrate analogues, *J. Biol. Inorg. Chem. 9*, 691−705.
20. Brenner, M. C., Zhang, H., and Scott, R. A. (1993) Nature of the low activity of S-methyl-coenzyme M reductase as determined by active site titrations, *J. Biol. Chem. 268*, 18491−18495.
21. Ellermann, J., Rospert, S., Thauer, R. K., Bokranz, M., Klein, A., Voges, M., and Berkessel, A. (1989) Methyl-coenzyme-M reductase from Methanobacterium thermoautotrophicum (strain Marburg). Purity, activity and novel inhibitors, *Eur. J. Biochem. 184*, 63−68.
22. Kunz, R. C., Horng, Y. C., and Ragsdale, S. W. (2006) Spectroscopic and kinetic studies of the reaction of bromopropanesulfonate with methyl-coenzyme M reductase, *J. Biol. Chem. 281*, 34663−34676.
23. Lahiri, G. K., and Stolzenberg, A. M. (1993) Facile formation of hexahydroporphyrin complexes by reduction of octaethylisobacteriochlorinnickel(II), *32*, 429−432.
24. Lin, S.-K., and Jaun, B. (1991) Coenzyme F430 from methanogenic bacteria: detection of a paramagnetic methylnickel(II) derivative of the pentamethyl ester by 2H-NMR spectroscopy, *Helv. Chim. Acta 74*, 1725−1738.
25. Lin, S.-K., and Jaun, B. (1992) Coenzyme F430 from methanogenic bacteria: mechanistic studies on the reductive cleavage of sulfonium ions catalyzed by F430 pentamethyl ester, *Helv. Chim. Acta 75*, 1478−1490.
26. Pelmenschikov, V., Blomberg, M. R., Siegbahn, P. E., and Crabtree, R. H. (2002) A mechanism from quantum chemical studies for methane formation in methanogenesis, *J. Am. Chem. Soc. 124*, 4039−4049.
27. Pelmenschikov, V., and Siegbahn, P. E. (2003) Catalysis by methyl-coenzyme M reductase: a theoretical study for heterodisulfide product formation, *J. Biol. Inorg. Chem. 8*, 653−662.
28. Zehnder, A. J. B., and Wuhrmann, K. (1976) Titanium(III) citrate as a nontoxic oxidation-reduction buffering system for the culture of obligate anaerobes, *Science 194*, 1165−1166.
29. Gunsalus, R. P., Romesser, J. A., and Wolfe, R. S. (1978) Preparation of coenzyme M analogues and their activity in the methyl coenzyme M reductase system of Methanobacterium thermoautotrophicum, *Biochemistry 17*, 2374−2377.
30. Bobik, T. A., and Wolfe, R. S. (1988) Physiological importance of the heterodisulfide of coenzyme M and 7-mercaptoheptanoylthreonine phosphate in the reduction of carbon dioxide to methane in Methanobacterium, *Proc. Natl. Acad. Sci. U.S.A. 85*, 60−63.
31. Noll, K. M., Donnelly, M. I., and Wolfe, R. S. (1987) Synthesis of 7-mercaptoheptanoylthreonine phosphate and its activity in the methylcoenzyme M methylreductase system, *J. Biol. Chem. 262*, 513−515.
32. Schonheit, P., Moll, J., and Thauer, R. K. (1979) Nickel, cobalt, and molybdenum requirement for growth of Methanobacterium thermoautotrophicum, *Arch. Microbiol. 123*, 105−107.
33. Ellermann, J., Hedderich, R., Bocher, R., and Thauer, R. K. (1988) The final step in methane formation. Investigations with highly purified methyl-CoM reductase (component C) from Methanobacterium thermoautotrophicum (strain Marburg), *Eur. J. Biochem. 172*, 669−677.
34. Dey, M., Telser, J., Kunz, R. C., Lees, N. S., Ragsdale, S. W., and Hoffman, B. M. (2007) Biochemical and Spectroscopic Studies of the Electronic Structure and Reactivity of a Methyl-Ni Species Formed on Methyl-Coenzyme M Reductase, *J. Am. Chem. Soc. 129*, 11030−11032.
35. Yang, N., Reiher, M., Wang, M., Harmer, J., and Duin, E. C. (2007) Formation of a nickel-methyl species in methyl-coenzyme M reductase, an enzyme catalyzing methane formation, *J. Am. Chem. Soc. 129*, 11028−11029.

BI701942W